ELSEVIER

In Collaboration with the Royal Netherlands Institute for Sea Research

Journal of Sea Research 52 (2004) 73–85

JOURNAL OF SEA RESEARCH

www.elsevier.com/locate/seares

Manganese oxide reactivity in North Sea sediments

Claar van der Zee*, Wim van Raaphorst[1]

Royal Netherlands Institute for Sea Research, Department of Marine Chemistry and Geology, P.O. Box 59, 1790 AB Den Burg, The Netherlands

Received 14 April 2003; accepted 17 October 2003

Abstract

Bulk Mn oxide dissolution rates were determined in dilute acid (HCl, pH 3, proton-assisted dissolution) and in saturating ascorbic acid (pH 3, proton-assisted plus reductive dissolution) for North Sea sediments from three sites characterised by different energy regimes, one at the Frisian Front, one in the German Bight, and one in the Skagerrak. Profiles of extractable manganese (0.1 N hydrochloric acid, 1 N hydrochloric acid, citrate-dithionite-bicarbonate buffer and hydroxylamine hydrochloride in acetic acid) are presented for the three sites.

The assemblage of sedimentary Mn oxides was described as a reactive continuum with a gamma distribution of Mn oxide reactivities. Initial reduction rates were highest for the oxidised sediment samples. The reactivity of the Mn assemblages during reductive dissolution in ascorbic acid decreased by up to ~9 orders of magnitude. The largest heterogeneity in Mn reactivity of the oxidised sediment samples was found at the German Bight site, while the most homogeneous Mn assemblage was found at the Skagerrak site. The large range in sedimentary Mn oxide reactivity may explain the great variability in values for kinetic coefficients used to describe Mn reduction. Considering the broad spectrum of Mn oxide reactivities, overlap of the Mn reduction zone with that of Fe oxides is expected.

Keywords: Manganese; Sediment; Early diagenesis; North Sea

1. Introduction

Manganese can be the most important intermediate oxidant between oxygen and organic carbon in marine sediments (Aller, 1990, 1994; Canfield et al., 1993; Thamdrup et al., 1994). A number of manganese oxides and oxyhydroxides (hereafter called Mn oxides) may exist in marine sediments with variable Mn (III) and Mn (IV) contents (Burdige, 1993). Below the depth of oxygen penetration in the sediment, Mn oxides are reductively dissolved thereby releasing Mn^{2+} into the pore water (Froelich et al., 1979; Burdige and Gieskes, 1983). Mn oxide reduction can be coupled to organic carbon oxidation (Myers and Nealson, 1988) and to the oxidation of reduced species such as dissolved ferrous iron (Postma, 1985) and sulphide (Burdige and Nealson, 1986). Microelectrode work showed field evidence consistent with the oxidation of Mn^{2+} by NO_3^- thereby producing N_2, whereas ammonium or organic nitrogen can reduce Mn oxides resulting in the production

---

* Corresponding author. Present address: Laboratory of Chemical Oceanography, Université Libre de Bruxelles, Campus de la Plaine, CP 208, Boulevard du Triomphe, 1050 Brussels, Belgium. Tel.: +32-2-6505218.

E-mail address: cvdzee@ulb.ac.be (C. van der Zee).

[1] Deceased.

1385-1101/$ - see front matter © 2004 Elsevier B.V. All rights reserved.
doi:10.1016/j.seares.2003.10.005

of N_2 as well (Luther et al., 1997). The rate of Mn reduction is affected by the reductant involved, microbial catalysis, and the mineralogy of the Mn oxide (Burdige et al., 1992). Mn reduction is a surface controlled process, and consequently amorphous manganese oxides with a larger specific surface area are generally reduced faster than highly crystalline oxides (Burdige et al., 1992). Dollhopf et al. (2000) showed that micro-organisms reduce Fe(III) electron acceptor phases with different kinetics: soluble Fe(III)-citrate faster than amorphous $Fe(OH)_3$, and that again faster than solid α-FeOOH. These findings suggest that different Mn electron acceptor phases are also likely to be reduced with different kinetics by bacteria. Also, the microbial community structure and viable cell numbers of relevant bacteria are important factors that affect the kinetics of metal oxide reduction (Dollhopf et al., 2000).

Natural marine Mn oxide phases are often intergrown with other materials and so poorly crystalline that their identification by x-ray diffraction techniques is very difficult (Burns and Burns, 1979). They deviate from pure minerals in their reactivity due to ionic substitution within the mineral and sorption of organic molecules and inorganic ions. Therefore, sediment extraction techniques are widely applied to marine sediments. Although these techniques are calibrated for iron phases (e.g. Canfield, 1988; Kostka and Luther, 1994; Haese et al., 1997), and much less for Mn phases (e.g. Chester and Hughes, 1967; Schenau, 1999), they are applied to both Mn and Fe. The disadvantage of extraction methods is that they are empirically defined and not mineral specific. Postma (1993) introduced a more quantitative method for natural sediments, based on the measurement of the rate of reductive dissolution of Fe oxides in ascorbic acid and using a reactive continuum model to describe the intrinsic reactivity of the assemblages of Fe-oxides.

Similarly, the reactivity of an assemblage of natural Mn oxides can be modelled as a reactive continuum, as was originally elaborated for organic matter degradation (Boudreau and Ruddick, 1991; Tarutis, 1993). The model has also been applied to the alkaline dissolution of biogenic silica (Koning et al., 1997). Based on the Gamma distribution of reactivities, the total amount of Mn oxides remaining, m (μmol g^{-1}), in a sample as a function of time, t (s), can be described by Eq. (1), where the mass at time zero is m_0. The parameter a (s) indicates the average lifetime of the reactive components in the mixture and υ is a dimensionless parameter solely related to the shape of the Gamma distribution curve.

$$\frac{m}{m_0} = \left(\frac{a}{a+t}\right)^{\upsilon} \tag{1}$$

The rate equation for Mn oxide dissolution is

$$J = k_m m^{1+\frac{1}{\upsilon}} \tag{2}$$

where J is the rate of dissolution (μmol g^{-1} s^{-1})

$$k_m = \frac{\upsilon}{a(m_0)^{1/\upsilon}} \tag{3}$$

Substitution of the rate constant k_m into (2) and rearranging gives

$$\frac{J}{m_0} = \frac{\upsilon}{a}\left(\frac{m}{m_0}\right)^{1+\frac{1}{\upsilon}} \tag{4}$$

Eq. (4) is similar to the general dissolution kinetics of a polydisperse sample of crystals (Eq. 5; Christoffersen and Christoffersen, 1976), in case of constant solution composition (i.e. constant concentration of reductant used). The parameter $k' = \upsilon/a$ (s^{-1}) represents the apparent rate constant.

$$\frac{J}{m_0} = k'\left(\frac{m}{m_0}\right)^{\gamma} \tag{5}$$

In this study, we present results on extraction methods and a reactive continuum approach applied to assemblages of natural Mn oxides in North Sea sediments. Three sites were selected on the basis of differences in their sediment reworking intensity. The objective was to investigate the effect of sediment reworking on the reactivity of natural marine Mn oxide assemblages. Sediment reworking affects the manganese redox cycling in sediments (Aller, 1990) and, thus, may affect the degree of ageing and reactivity of the sedimentary Mn oxides. The second objective was to quantify the range of Mn oxide reactivities encountered in one assemblage. This may at least partly explain the large variability found in kinetic coefficients of Mn reduction (Burdige and

Gieskes, 1983; Van Cappellen and Wang, 1996; Slomp et al., 1997; Boudreau et al., 1998; Van der Zee et al., 2001). Insight into the Mn reactive continuum will provide constraints on the kinetic coefficients and thus improve modelling of the Mn cycle. As the stability of Mn oxides in natural sediments is roughly paralleled by their reactivity, a heterogeneous assemblage of Mn oxides may cause an extensive overlap between the Mn reduction zone with that of the Fe oxides.

2. Methods

2.1. Research area

Three sites in the North Sea representing different energy regimes were visited with RV 'Pelagia' in November 1995 (Fig. 1; Table 1). The relatively deep and sheltered Skagerrak was selected as a low-energy site characterised by a steady sedimentation of relatively refractory organic matter from the Scandinavian mainland, the Baltic and particularly from the North Sea shelf (Van Weering et al., 1987). The low food quality of the organic matter (Dauwe et al., 1999) is reflected in the relatively low biomass and the very small mean individual weight of the macrofauna (Dauwe et al., 1998).

Table 1
Name, geographical position, water depth, bottom water temperature of stations

Station	N	E	Depth (m)	BW Temp (°C)
Frisian Front	53° 42′	04° 30′	39	13
German Bight	54° 05′	08° 09′	20	10
Skagerrak	58° 12′	10° 15′	270	7.2

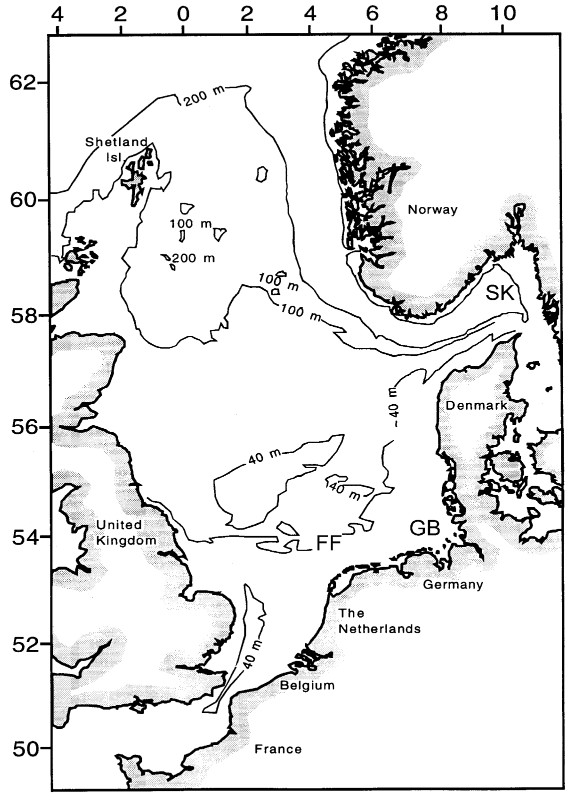

Fig. 1. Map of the North Sea and the stations (FF, GB and Sk).

In contrast to the Skagerrak, two shallow and highly dynamic areas were sampled, the moderately energetic site in the Frisian Front and the highly energetic site in the German Bight. Particles from the East Anglian turbidity plume and the south-western North Sea settle in the Frisian Front area in spring and summer (Puls and Sündermann, 1990; Sündermann, 1993; Van Raaphorst et al., 1998); however, these particles are eroded again during autumn and winter storms (Kempe et al., 1988; Puls and Sündermann, 1990). The sediment consists of old reworked deposits partly mixed with recent sediments (De Haas et al., 1997). In contrast to the vertically homogenous sediment column of the Skagerrak, a distinct layer with fine particles, median grain size ~30 μm, was present between ~1.5 and 5 cm depth at the Frisian Front. Above and below this layer, the particles were coarser with a median grain size of ~100 μm (Van der Zee et al., 2003). The upper 10 cm of the sediment in the German Bight consisted of 6 alternating fine- and coarse-particle layers with median grain sizes varying between ~30 and 90 μm (Van der Zee et al., 2003). Strongly variable tidal currents resuspend the surface sediment at the German Bight regularly (Boon and Duineveld, 1996). Physical and biological sediment reworking stimulates Mn cycling in these dynamic areas (Van der Zee et al., 2003).

2.2. Sediment handling

Sediment samples were taken with a multi-corer and processed immediately upon retrieval onboard.

All subsequent sediment handling took place at in situ temperature. Cores were sliced in four 2.5-mm intervals (0–2.5, 2.5–5, 5–7.5 and 7.5–10 mm), four 5-mm intervals (10–15, 15–20, 20–25 and 25–30 mm), four 10-mm intervals (30–40, 40–50, 50–60 and 60–70 mm) and two 15-mm intervals (70–85, 85–100 mm). Sediment slices of 4 cores were pooled and centrifuged (10 min, 3000 rpm). Pore water was collected after centrifugation and filtered (0.45 μm, Acrodisc). Aliquots for manganese were acidified to pH ~ 1 and measured on a TRAACS-800 auto-analyser according to the method Brewer and Spencer (1971). After pore water collection, the sediment was stored frozen (−20 °C) until solid phase analysis in the NIOZ laboratory. Freeze-dried and ground (Teflon mortar and pestle) sediment was extracted for Mn at room temperature with 1 N HCl for 24 h (Slomp et al., 1997), 0.1 N HCl for 18 h (Duinker et al., 1974), 1M Hydroxylamine hydrochloride in 25% (v/v) acetic acid for 1 h (HA.AA, Chester and Hughes, 1967), and Citrate-Dithionite-Bicarbonate for 8 h at pH 7.3 (CDB, Ruttenberg, 1992). Wet chemical extractions are operationally defined and only moderately selective. Therefore the results should be interpreted with caution. Both 1 N and 0.1 N HCl will dissolve carbonate phases and extract some Mn oxides, where 0.1 N HCl is assumed to extract the same phases as 1 N HCl but with less attack on clay minerals (Duinker et al., 1974; Slomp et al., 1997). The CDB extraction was developed to reductively dissolve Fe oxides without dissolution of carbonate phases (Ruttenberg, 1992). Thus, CDB-extractable Mn is not expected to include any Mn originating from carbonate phases. Finally, HA.AA extracts all Mn in oxides and carbonates (Chester and Hughes, 1967).

2.3. Dissolution experiments

The top (0–0.25 cm) and bottom (8.5–10 cm) layers of the three stations and the Mn oxide maximum (0.75–1 cm) layer of the German Bight were used in proton-assisted and reductive dissolution experiments. Postma (1993) used ascorbic acid as reductant in his Fe oxide dissolution experiments and it is a suitable reductant for Mn oxides as well. It dissolved Mn (III) and (IV) oxides at pH 7.2 as quickly as any of the 27 aromatic and non-aromatic compounds tested by Stone and Morgan (1984). The Mn oxide dissolution experiments were carried out with excess ascorbic acid, following Postma (1993), so that the rate is independent of the reductant concentration, which does not change appreciably over time. The reductive dissolution experiment started by adding sediment (~ 1 g) to 250 ml freshly prepared 10 mM ascorbic acid solution (pH 3). The suspension was stirred continuously to prevent the particles settling and kept at constant pH 3.0 ± 0.1 by adding 1 N HCl. Aliquots of the suspension were filtered (0.2 μm), acidified to pH ~ 1 and measured for Mn^{2+} by flame AAS. Postma (1993) found that in the presence of only HCl at pH 3 less than 1% of ferrihydrite dissolved in ~ 5 h. In order to test proton-assisted manganese dissolution at pH 3, an additional experiment was carried out in a HCl solution at pH 3.0 ± 0.1. Aliquots of the suspension were filtered (0.2 μm), acidified to pH ~ 1 and measured on a TRAACS-800 auto-analyser according to the method Brewer and Spencer (1971).

The released Mn^{2+} (in μM) normalised to the added amount of sediment (g) and volume of ascorbic acid or HCl solution (L) results in a dissolution curve of released Mn^{2+} in μmol g^{-1} versus time. The amount of released Mn^{2+} is equal to the m_0 (μmol g^{-1}), when no further dissolution occurs. The amount of Mn oxides remaining, m, is the difference between m_0 and the amount of released Mn^{2+} at time t. Sums of squares were minimised while the parameters a, υ and m_0 were varied to fit Eq. (1) to the dissolution data using the Excel solver routine.

3. Results

3.1. Manganese profiles

At the Frisian Front site, Mn profiles from the 0.1 N HCl, 1 N HCl and HA.AA extractions are almost identical, whereas CDB-extractable Mn shows a similar depth distribution but with a lower concentration, offset ~ 1 μmol Mn g^{-1} (Fig. 2). The pore water profile shows that Mn oxide is reduced between ~ 1 and 2 cm depth and the re-oxidation of dissolved Mn^{2+} upon diffusion into the upper cm of the sediment. At the German Bight site, the HA.AA, 0.1 N and 1 N HCl solutions dissolve similar amounts of Mn, except in the subsurface maximum (~ 1 cm

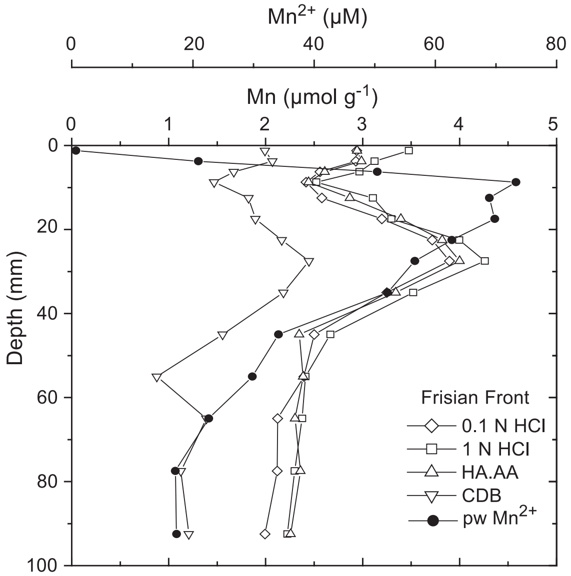

Fig. 2. Vertical profile of pore water Mn^{2+} (solid circles) and Mn extracted with 0.1 N HCl (square), 1 N HCl (open circle), HA.AA (up triangle) and CDB (down triangle) at the Frisian Front.

depth), where more Mn is dissolved by HA.AA (Fig. 3). At the Frisian Front site, CDB extracts the least amount of Mn. The pore water profile of Mn^{2+} shows that Mn reduction takes place around 1 cm depth and that dissolved Mn^{2+} is re-oxidised in the upper half cm of the sediment. Mn^{2+} is precipitated as a reduced Mn phase below 1.5 cm depth, unless the decrease with depth of Mn^{2+} is due to intense pore water irrigation. At the Skagerrak site, 1 N HCl extracts most and CDB least Mn (Fig. 4). Again, the vertical distribution is the same for all extractions. Mn oxide is reduced between 2–3 cm depth and Mn^{2+} is re-oxidised at the sediment-water interface, which is visible as an enrichment of extractable Mn in the surface sediment.

3.2. Reactive continuum approach

During the dissolution experiments, a fast initial release of Mn^{2+} is observed that strongly decelerates when the major part of the Mn oxide assemblage is dissolved (Fig. 5). The fraction of Mn oxide remaining during the reduction by ascorbic acid and proton-assisted dissolution can be well described by the reactive continuum as shown by the model fit to the dissolution curves (Fig. 5). Fitted values (a, υ and m_0) are given as υ/a and $1 + 1/\upsilon$ in Table 2 and m_0 in Table 3. The fitted m_0 values are thus ascorbic acid-extract-

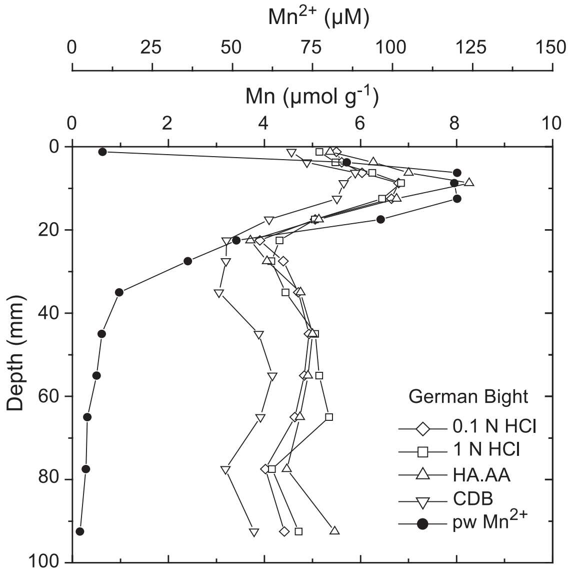

Fig. 3. Vertical profile of pore water Mn^{2+} (solid circles) and Mn extracted with 0.1 N HCl (square), 1 N HCl (open circle), HA.AA (up triangle) and CDB (down triangle) at the German Bight.

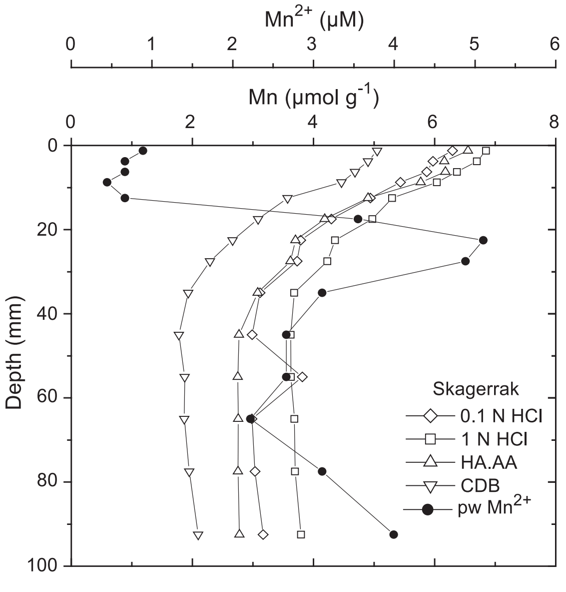

Fig. 4. Vertical profile of pore water Mn^{2+} (solid circles) and Mn extracted with 0.1 N HCl (square), 1 N HCl (open circle), HA.AA (up triangle) and CDB (down triangle) at the Skagerrak.

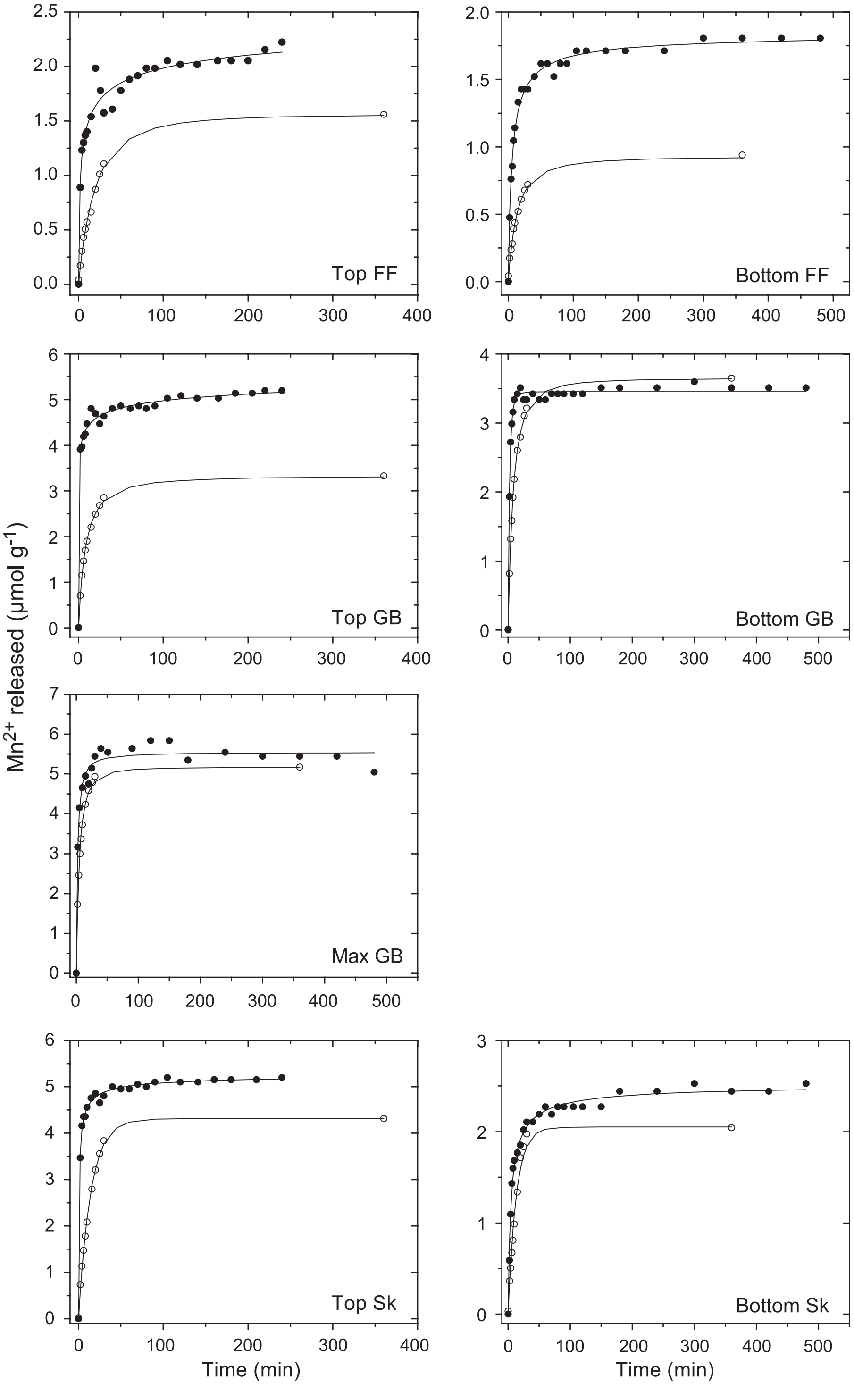

Fig. 5. The Mn^{2+} release per gram sediment during the dissolution of natural Mn oxides in 10 mM ascorbic acid (solid circles) and HCl solution (open circles) at pH 3. The line represents the fit of Eq. 1 to the data.

able and HCl pH 3-exctractable m_0 values, respectively, and are comparable to the Mn concentrations obtained with the CDB, HA.AA and 1 N and 0.1 N HCl extractions (Table 3) suggesting that the model parameter estimates are realistic. The HCl (pH 3) m_0 values in the top layers are comparatively low, however. Its comparison with the Mn concentrations of the four extracts is complicated by differences in extraction time, pH, extracted Mn phases and dissolution mechanism, e.g. proton-assisted or reductive dissolution or a combination of both.

The constant term υ/a in Eq. 4 can be regarded as an apparent rate constant (k') for the reductive dissolution of a natural Mn oxide mixture with 10 mM ascorbic acid or proton-assisted dissolution in HCl at pH 3.0 and room temperature. For an ideal dissolving cube or sphere γ (Eq. 5) is 0.67 predicted by the relation between volume and surface area. In natural samples, the exponential term $1 + 1/\upsilon$ cannot be interpreted in physical terms, but it is characteristic of the reactivity of the oxides present; a higher exponential term indicates a larger range of Mn reactivities (Postma, 1993). The reactivity is not only related to the mineralogy, but also to the crystal geometry, particle size distribution and reactive site density (Burdige et al., 1992; Postma, 1993; Larsen and Postma, 2001). The estimated rate constants and exponential terms are both higher in the top sediments than in the bottom sediments for ascorbic acid (Table 2). The higher rate constant indicates a higher initial reduction rate and the higher exponential term indicates a wider range of Mn oxide reactivities in the oxic top layer of the sediment. The estimated rate constants in the HCl (pH 3) dissolution experiments are always lower than the corresponding rate constants found in the dissolution experiments with ascorbic acid. The differences are most pronounced in the top layers, whereas only small differences are found in the subsurface and bottom layers. The estimated exponents in the HCl (pH 3) experiment are low and very similar between top and bottom sediments from each station.

Table 2
Values obtained by fitting Eq. (1) to the dissolution curves of Mn^{2+} in ascorbic acid and HCl (pH 3)

Sample	Constant (υ/a) (s^{-1}) ascorbic acid	exponent ($1 + 1/\upsilon$) (−) ascorbic acid	constant (υ/a) (s^{-1}) HCl	exponent ($1 + 1/\upsilon$) (−) HCl
FF-0–0.25 cm	9.9 E-3	5.8	8.7 E-4	1.4
FF-8.5–10 cm	3.3 E-3	2.4	1.3 E-3	1.7
GB-0–0.25 cm	8.9 E-1	8.9	2.0 E-3	1.7
GB-0.75–1 cm	8.0 E-3	1.8	3.2 E-3	1.5
GB-8.5–10 cm	7.7 E-3	1.3	2.0 E-3	1.5
Sk-0–0.25 cm	2.9 E-2	2.8	1.2 E-3	1.0
Sk-8.5–10 cm	3.8 E-3	2.4	1.3 E-3	1.0

Table 3
Mn (μmol g^{-1}) values obtained by fitting Eq. (1) to the dissolution curves and the amount of Mn extracted with 0.1 N HCl, 1 N HCl, CDB and HA.AA

Sample	m_0 ascorbic acid	m_0 HCl (pH 3)	0.1 N HCl	1 N HCl	CDB	HA.AA
FF-0–0.25 cm	2.4	1.6	2.9	3.5	2.0	2.9
FF-8.5–10 cm	1.8	0.9	2.0	2.2	1.2	2.3
GB-0–0.25 cm	5.6	3.3	5.5	5.1	4.6	5.4
GB-0.75–1 cm	5.5	5.2	5.6	5.5	4.9	6.3
GB-8.5–10 cm	3.5	3.6	4.4	4.7	3.8	5.5
Sk-0–0.25 cm	5.3	4.3	6.3	6.9	5.1	6.6
Sk-8.5–10 cm	2.6	2.1	3.2	3.8	2.1	2.8

4. Discussion

4.1. Classical extractions

The CDB extraction did leach less Mn from the sediments than HCl and HA.AA, probably because Mn in carbonates is not dissolved in the ~neutral CDB solution. The 0.1 N HCl solution always extracts less Mn than 1 N HCl, suggesting that Mn is leached preferentially from clay minerals in HCl. At the Skagerrak site, a Mn oxide enrichment at the sediment surface is visible, in contrast to the Frisian Front and German Bight sites. The vertical distribution of solid phase and pore water Mn is governed by physical and biological mixing events at the Frisian Front and German Bight (Van der Zee et al., 2003). After a perturbation the pore water distributions adjust rapidly, whereas the solid phase exhibits a transient profile for a longer period. As a result, depth distributions of 1 N HCl extractable Mn in sediments of the Frisian Front site and especially the German Bight site measured in different months (February, May, August and November) are very different (Van der Zee et al., 2003).

Features of several solid phase depth distributions (Mn, Fe, C_{org}) are also encountered in the same seasons but in other years for these sites (Van Raaphorst et al., 1992; Slomp et al., 1997), suggesting that the underlying processes are not accidental and seasonally reoccurring. Thus, the cores are representative of the sites in these particular seasons.

The pore water Mn^{2+} profiles suggest the formation of a reduced authigenic Mn mineral. Precipitation of Mn in calcium carbonates is not visible, however, in the solid Mn profiles as the difference between HA.AA, 0.1 N HCl or 1 N HCl and CDB extractable Mn does not increase at depth, where the dissolved Mn^{2+} starts to decrease. Alternatively, the profiles may still be relaxing from a non-steady state in case of the Frisian Front and German Bight or we may see the effect of irrigation. The difference between Mn extractable in CDB and the other extractants may point at a constant 'background' concentration of Mn in calcium carbonates or silicates. Few differences are observed between the various extractions and their depth distributions.

4.2. Reactive continuum approach: the initial rates

The ascorbic acid dissolution is used to quantify the Mn oxide reactivity, because it combines proton-assisted and reductive dissolution. Therefore this experiment will be discussed in more detail than the HCl experiment, which only serves as a comparison to the ascorbic acid dissolution. For iron oxides proton-assisted dissolution is usually the slowest of the oxide dissolution pathways, while the presence of a ligand increases the rate, but dissolution is fastest in the presence of a reductant such as ascorbic acid (e.g. Schulzberger et al., 1989; Stumm and Schulzberger, 1992). This is consistent with the observation of Postma (1993) that no more than 1% of the ferrihydrite dissolves in HCl solution (pH 3). The substantial dissolution of Mn in dilute HCl (pH 3), however, suggests that proton-assisted dissolution is of importance for Mn, as was also suggested by the classical extractions discussed earlier. Mn dissolution in dilute HCl may not be true proton-assisted dissolution, because the acid can liberate Fe^{2+} and organics that reductively dissolve Mn. Nevertheless, the difference between the two experiments is due to the reductive power of ascorbate and therefore solely represents Mn(III) and Mn(IV). Dissolution of Mn from carbonates or silicates due to the solution pH (3.0) is the same for both ascorbate and dilute HCl.

The dissolution rates of the different samples are plotted in Fig. 6a as $-\log(J/m_0)$ versus $-\log(m/m_0)$ to compare their Mn oxide reactivities. At time zero, the reaction rate J normalised to m_0 equals υ/a, which is the apparent rate constant, k' (Fig. 6a). On the x-axis, increasing values indicate decreasing amounts of Mn oxides remaining as dissolution proceeds. In the sediment, reduction rates also depend on factors such as the specific reductant involved and pH, bacterial community structure and number of viable cells (Doll-

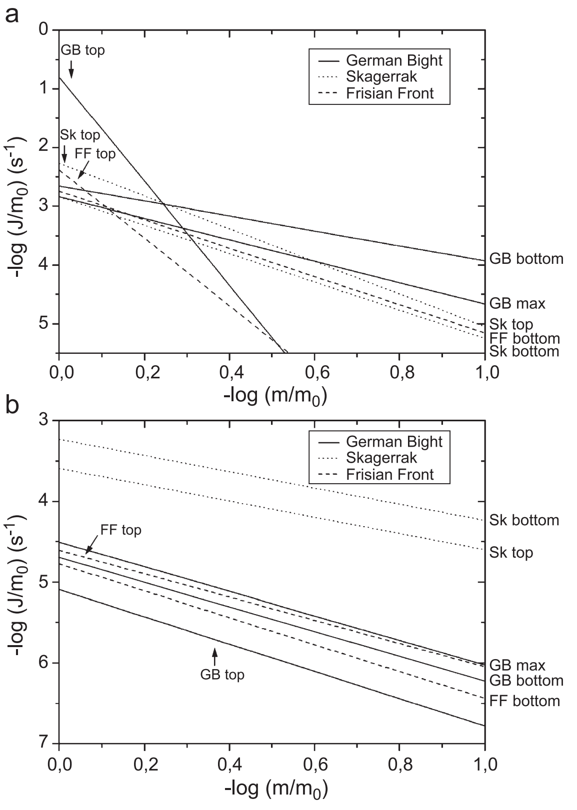

Fig. 6. (a) Mn oxide reduction rates in ascorbic acid (pH 3) solution normalised to the initial mass (J/m_0) versus the fraction (m/m_0) remaining in the solid phase of the top and bottom samples of the Frisian Front (dashed lines), German Bight (solid lines), and Skagerrak (dotted lines). (b) Mn oxide reduction rates in HCl (pH 3) solution normalised to the initial mass (J/m_0) versus the fraction (m/m_0) remaining in the solid phase of the top and bottom samples of the Frisian Front (dashed lines), German Bight (solid lines), and Skagerrak (dotted lines).

hopf et al., 2000), but the dissolution rates estimated in the experiments are a function of the Mn oxide reactivity only in this case. The rate is independent of the ascorbic acid concentration, because it does not change appreciably over time. The initial dissolution rates ($J\ m_0^{-1}$) roughly range between 10^{-3} and 10^{0} (s^{-1}) in ascorbic acid and between 10^{-6} and 10^{-3} (s^{-1}) in HCl (Fig. 6b), showing the difference in reductive plus proton-assisted dissolution versus proton-assisted dissolution alone (Fig. 6a, b). At the same pH, Mn oxides will dissolve faster in the presence of a reductant such as ascorbic acid.

The three oxidised surface sediment samples have the highest initial dissolution rates in ascorbic acid (Fig. 6a). The variation of the initial rates over more than 2 orders of magnitude indicates that large differences in the most reactive Mn oxide phase exist between the different marine sediments. The variation is greatest among the top sediments (2 orders of magnitude) and much smaller among the bottom samples (half an order of magnitude). The German Bight is an area of intense cycling apparently containing very reactive Mn oxides as suggested by the very high initial dissolution rate in the top sample.

4.3. Reactive continuum approach: the range of reactivities

The negative slopes of the lines in Fig. 6a reflect the decrease in dissolution rate. The three oxidised surface sediment samples have the largest range of reactivities. The bottom samples, from the reduced sediment layer, have much smaller ranges of reactivities, i.e. the lines are more horizontally oriented. Deeper in the sediment, the Mn pool becomes more homogeneous probably leaving only the very resistant Mn oxides to be buried together with detrital Mn in clay minerals and reduced authigenic phases. The decrease in reactivity during dissolution in ascorbic acid can span several orders of magnitude suggesting an enormous heterogeneity in Mn oxide reactivity, especially for the top sediments of the highly energetic German Bight (~9 orders of magnitude) and the moderately energetic Frisian Front (~6 orders of magnitude). In contrast, the oxidised top sample from the Skagerrak is relatively homogeneous (~3 orders of magnitude variation). Thus, most heterogeneous Mn oxide assemblages are found in more intensely reworked sediments. Postma (1993) found a change in reactivity of the ferric oxides of almost 5 orders of magnitude in Aarhus Bight sediment. The reactivity of the subsurface maximum at the German Bight site is similar to that of the bottom sample, thus the most reactive Mn is already dissolved in the upper zone of Mn reduction.

The difference between dissolution by ascorbic acid and HCl (Table 2) is large in the top layers, where the Mn oxide heterogeneity is large. For the bottom layers, however, the difference is very small. The bottom layer sediment has already passed the Mn reduction zone, so the major part of the ‘easily reducible’ Mn oxides should be gone. This effect is reflected in the smaller difference between the reductive plus proton-assisted dissolution (ascorbic acid) and the proton-assisted only dissolution (HCl) in the deeper layers. Suppose that in the bottom layers Mn is associated with carbonates only and the difference between HCl and ascorbic acid in the top layers represents additional Mn oxides. The amount of Mn extracted in the bottom layers would then equal the difference between HA.AA and CDB extractable Mn, which is 1.1 μmol Mn g^{-1} at the Frisian Front site, 1.7 μmol Mn g^{-1} at the German Bight site and 0.7 μmol Mn g^{-1} at the Skagerrak site. The fitted m_0 for Mn dissolution in HCl (pH 3) is 0.9 μmol Mn g^{-1} at the Frisian Front site, 3.6 μmol Mn g^{-1} at the German Bight site and 2.1 μmol Mn g^{-1} at the Skagerrak site. Thus, at the Frisian Front site it is possible that HCl at pH 3 only extracted Mn associated with carbonates. At the German Bight and Skagerrak sites, however, twice that amount was extracted with HCl at pH 3. Thus, the differences between top and bottom layers more likely reflect the differences between the Mn oxide assemblage before and after Mn reduction.

4.4. Mn oxidation products/heterogeneity

Hem and Lind (1983) argued that in aerated aqueous systems the initial Mn^{2+} oxidation product would be a metastable solid species with the Mn oxidation number no greater than +3.0. Depending on the ionic medium and the reaction temperature several Mn oxidation products may form (Hem and Lind, 1983). Conditions favourable for the development of Mn (IV) oxides (MnO_2) are most likely to occur when the initial precipitate is β-MnOOH (feithknechtite). However, if the initial product is Mn_3O_4

(hausmannite), it will transform into γ-MnOOH (manganite), which is more stable than β-MnOOH and is not altered to more oxidised forms within a period of several months (Hem and Lind, 1983; Murray et al., 1985). Microbial Mn^{2+} oxidation can result in various oxidation products as well. Bacterial spores of the marine *Bacillus* strain SG-1 can directly oxidise Mn (II) to Mn (IV) without the formation of Mn (III) intermediates (Mandernack et al., 1995). The biogenic Mn oxides produced by the bacterium *Leptothrix discophora* SS-1, however, were shown to be mixed Mn (III, IV) oxides with an average oxidation state of 3.6 and a rather high surface area of 224 m^2 g^{-1} implying a high reactivity (Nelson et al., 1999; Adams and Ghiorse, 1988). Based on these experiments, a wide range of Mn reactivities can be expected in the oxic layer of the sediment. Both freshly precipitated Mn (III) oxides with a high reactivity and more aged crystalline Mn (IV) oxides with a lower reactivity are likely to occur. This is consistent with the large heterogeneity found in the oxidised surface samples. Some field investigations do not suggest a large mineralogical diversity in marine and lake sediments (e.g. Canfield et al., 1993; Friedl et al., 1997). Even if this is so, a range of reactivities is likely in natural sediments, because the reactivity of a single mineral depends greatly on its particle size distribution, crystal morphology and reactive site density (Larsen and Postma, 2001).

The Mn oxide heterogeneity in the top layer increases with physical sediment mixing intensity. The Mn^{2+} ions experience a variable chemical environment (e.g. Luther et al., 1997; Huettel et al., 1998), which results in different oxidation products and thus, a large heterogeneity. In contrast to biodiffusional mixing, which tends to flatten concentration profiles, the physical perturbations that mix the sediments of the Frisian Front and German Bight sites result in a layering of the sediment. Therefore these perturbations increase the sedimentary heterogeneity instead of homogenising the sediments.

4.5. Manganese cycling

Diagenetic models generally describe sediment profiles of Mn oxides and dissolved Mn^{2+} rather well (e.g. Burdige and Gieskes, 1983; Van Cappellen and Wang, 1996; Slomp et al., 1997; Boudreau et al., 1998; Van der Zee et al., 2001). Large variations in kinetic coefficients are found in these studies, however, because a number of processes are lumped into one single rate constant. The Mn reduction rate depends on several factors, e.g. Mn oxide reactivity, temperature, bacterial versus inorganic catalysis, organic matter reactivity, and the type of reductant involved (e.g. Burdige and Gieskes, 1983; Slomp et al., 1997). Considering the large variation in Mn reactivity found in this study, this could be one of the major factors determining these large variations in kinetic coefficients. In the sediment, the most reactive Mn oxides will be reduced preferentially leaving more resistant Mn oxides behind. The Mn reduction rate will decrease upon removal of the most reactive Mn oxides. Therefore Mn cycling is most intense close to the Mn redox boundary, where Mn reactivity is largest.

The reactive continuum approach offers the possibility to compare the intrinsic Mn reactivity in a standardised way, which can be used to assess the rate limiting factors for Mn reduction and its contribution to total carbon mineralisation. Previously, the relatively low concentration of sedimentary Mn oxides was suggested to limit the contribution of Mn reduction to overall carbon mineralisation (Bender and Heggie, 1984). However, the Mn oxide concentration is not per se rate limiting for the Mn reduction rate, due to rapid recycling. Manganese is an efficient electron shuttle between oxygen and organic matter, through re-oxidation of Mn^{2+} by molecular oxygen (Aller, 1994). The Mn oxide reactivity likely affects the microbial Mn reduction rate as has been shown for Fe (Dollhopf et al., 2000) and thus Mn cycling in aquatic sediments.

4.6. Redox zonation

Depending on their free energy yield and availability, a suite of electron acceptors is used in the degradation of organic matter, oxygen, nitrate, Mn oxides, Fe oxides and sulphate (Froelich et al., 1979). The reactivity of Fe oxides in natural sediments varies over orders of magnitude (Postma, 1993) and their reactivity is roughly paralleled by their instability (Dos Santos Afonso and Stumm, 1992). Postma and Jakobsen (1996) argued therefore that due to the large variability in Fe oxides present in marine sediments, Fe reduction is favoured in the presence of amorphous Fe hydroxides, but as the stability of the Fe oxide increases, sulphate reduction becomes the favourite pathway for organic-matter degradation. Similar to the Fe oxides, the bulk dissolution experiments show that natural Mn oxides are present in widely variable reactivities. Analogous to the iron-sulfate equilibrium, the nitrate-manganese redox equilibrium strongly depends on the stability of the Mn oxides present in the sediment. Although one may argue that synthetic Mn oxides, even the amorphous, are not the same as natural amorphous Mn oxides, nitrate reduction appears to be favoured over amorphous Mn oxide reduction, because bacteria prefer a soluble electron acceptor to a solid form (Dollhopf et al., 2000). Considering the enormous range of reactivities found for both Mn oxides and Fe oxides in natural sediments, vertical overlap of the metal reduction zones can be expected. Some Mn oxides may escape reduction and be buried, when the Fe oxides are more reactive. The solid Mn profiles do suggest that Mn oxides are present below the Mn reduction zone. In the Skagerrak, for example, ~40% of the CDB-extractable Mn of the top layer is preserved at 10 cm depth.

5. Conclusions

The application of the reactive continuum approach provides more information on the Mn reactivity than conventional extraction methods do. It can be useful in the interpretation of Mn profiles from energetic environments such as the German Bight and Frisian Front, which are difficult to interpret from the depth distributions only. Large differences in the most reactive Mn oxide phase exist between the oxidised surface sediments of the three sites. The differences between sites in the deeper anoxic sediments, however, are much smaller. The heterogeneity of the natural assemblage of Mn oxides may increase with physical sediment mixing intensity. The homogeneous assemblage of Mn oxides in the reduced sediment samples suggests that some Mn oxides escape reduction in the sediment. Considering the variability in reactivity found for both Mn oxides and Fe oxides in natural sediments, vertical overlap of metal reduction zones can be expected.

Acknowledgements

We thank the captain, crew and scientific party of the RV 'Pelagia' for their help. Karel Bakker and Jan van Ooyen performed the Mn^{2+} analyses (Dept. Marine Chemistry and Geology, NIOZ). Critical comments by Philippe van Cappellen and Eric Epping on earlier drafts of the manuscript were much appreciated. C.v.d.Z. was supported through a grant to W.v.R. from the Netherlands Organisation for Scientific Research (NWO) SMILE program (no. 750.297.01). C.v.d.Z. is presently a research fellow supported by the Belgian Federal Office for Scientific, Technical and Cultural Affairs (contract no. EV/11/20B).

References

Adams, L.F., Ghiorse, W.C., 1988. Oxidation state of Mn in the Mn oxide produced by *Leptothrix discophora* SS-1. Geochim. Cosmochim. Acta 52, 2073–2076.

Aller, R.C., 1990. Bioturbation and manganese cycling in hemipelagic sediments. Phil. Trans. R. Soc. London A 331, 51–68.

Aller, R.C., 1994. The sedimentary Mn cycle in Long Island Sound: Its role as intermediate oxidant and the influence of bioturbation, O2, and Corg flux on diagenetic reaction balances. J. Mar. Res. 52, 259–295.

Bender, M.L., Heggie, D.T., 1984. Fate of organic carbon reaching the deep sea floor: a status report. Geochim. Cosmochim. Acta 48, 977–986.

Boon, A.R., Duineveld, G.C.A., 1996. Phytopigments and fatty acids as molecular markers for the quality of near bottom particulate organic matter in the North Sea. J. Sea Res. 35, 279–291.

Boudreau, B.P., Ruddick, B.R., 1991. On a reactive continuum representation of organic matter diagenesis. Am. J. Sci. 291, 507–538.

Boudreau, B.P., Mucci, A., Sundby, B., Luther, G.W., Silverberg, N., 1998. Comparative diagenesis at three sites on the Canadian continental margin. J. Mar. Res. 56, 1259–1284.

Brewer, P.G., Spencer, D.W., 1971. Colorimetric determination of manganese in anoxic waters. Limnol. Oceanogr. 16, 107–110.

Burdige, D.J., 1993. The biogeochemistry of manganese and iron reduction in marine sediments. Earth Sci. Rev. 35, 249–284.

Burdige, D.J., Gieskes, J.M., 1983. A pore water/solid phase diagenetic model for manganese in marine sediments. Am. J. Sci. 283, 29–47.

Burdige, D.J., Nealson, K.H., 1986. Chemical and microbial studies of sulfide-mediated manganese reduction. Geomicrobiol. J. 4, 361–387.

Burdige, D.J., Dhakar, S.P., Nealson, K.H., 1992. Effects of manganese oxide mineralogy on microbial and chemical manganese reduction. Geomicrobiol. J. 10, 27–48.

Burns, R.G., Burns, V.M., 1979. Manganese oxides. In: Burns, R.G. (Ed.), Marine Minerals. Reviews in Mineralogy, vol. 6. Mineralogy Society of America, Washington, DC, pp. 1–46.

Canfield, D.E., 1988. Sulfate reduction and the diagenesis of iron in anoxic marine sediments. Ph.D. Thesis. Yale University.

Canfield, D.E., Thamdrup, B., Hansen, J.W., 1993. The anaerobic degradation of organic matter in Danish coastal sediments: iron reduction, manganese reduction and sulfate reduction. Geochim. Cosmochim. Acta 57, 3867–3883.

Chester, R., Hughes, M.J., 1967. A chemical technique for the separation of ferro-manganese minerals, carbonate minerals and adsorbed trace elements from pelagic sediments. Chem. Geol. 2, 249–262.

Christoffersen, J., Christoffersen, M.R., 1976. The kinetics of dissolution of calcium sulphate dihydrate in water. J. Crystal Growth 35, 79–88.

Dauwe, B., Herman, P.M.J., Heip, C.H.R., 1998. Community structure and bioturbation potential of macrofauna at four North Sea stations with contrasting food supply. Mar. Ecol. Prog. Ser. 173, 67–83.

Dauwe, B., Middelburg, J.J., Van Rijswijk, P., Sinke, J., Herman, P.M.J., Heip, C.H.R., 1999. Enzymatically hydrolyzable amino acids in North Sea sediments and their possible implication for sediment nutritional values. J. Mar. Res. 57, 109–134.

De Haas, H., Boer, W., Van Weering, T.C.E., 1997. Recent sediment and organic carbon burial in a shelf sea; the North Sea. Mar. Geol. 144, 131–146.

Dollhopf, M.E., Nealson, K.H., Simon, D.M., Luther III, G.W., 2000. Kinetics of Fe(III) and Mn(IV) reduction by the black sea strain of *Shewanella putrefaciens* using in situ solid state voltametric Au/Hg electrodes. Mar. Chem. 70, 171–180.

Dos Santos Afonso, M., Stumm, W., 1992. Reductive dissolution of iron (III) (hydr)oxides by hydrogen sulfide. Langmuir 8, 1671–1675.

Duinker, J.C., Van Eck, G.T.M., Nolting, R.F., 1974. On the behaviour of copper, zinc, iron and manganese, and evidence for mobilization processes in the Dutch Wadden Sea. Neth. J. Sea Res. 8, 214–239.

Friedl, G., Werhli, B., Manceau, A., 1997. Solid phases in the cycling of manganese in eutropic lakes: new insights from EXAFS spectroscopy. Geochim. Cosmochim. Acta 61, 275–290.

Froelich, P.N., Klinkhammer, G.P., Bender, M.L., Luedtke, N.A., Heath, G.R., Cullen, D., Dauphin, P., Hammond, D., Hartman, B., Maynard, V., 1979. Early oxidation of organic matter in pelagic sediments of the eastern equatorial Atlantic: suboxic diagenesis. Geochim. Cosmochim. Acta 43, 1075–1090.

Haese, R.R., Wallman, K., Dahmke, A., Kretzmann, U., Müller, P.J., Schulz, H.D., 1997. Iron species determination to investigate early diagenetic reactivity in marine sediments. Geochim. Cosmochim. Acta 61, 63–72.

Hem, J.D., Lind, C.J., 1983. Nonequilibrium models for predicting forms of precipitated manganese oxides. Geochim. Cosmochim. Acta 47, 2037–2046.

Huettel, M., Ziebis, W., Forster, S., Luther III, G.W., 1998. Advective transport affecting metal and nutrient distributions and interfacial fluxes in permeable sediments. Geochim. Cosmochim. Acta 62, 613–631.

Kempe, S., Liebezeit, G., Dethlefsen, V., Harms, U., 1988. Biogeochemistry and distribution of suspended matter in the North Sea and implications to fisheries biology. Syn. Mitt. Geol.-Paläont. Inst. Univ. Hamburg, SCOPE/UNEP, Sonderband 65, XI–XXIV.

Koning, E., Brummer, G.-J., Van Raaphorst, W., Van Bennekom, J., Helder, W., Van Iperen, J., 1997. Settling, dissolution and burial of biogenic silica in the sediments off Somalia (northwestern Indian Ocean). Deep-Sea Res. II 44, 1341–1360.

Kostka, J.E., Luther III, G.W., 1994. Partitioning and speciation of solid phase iron in saltmarsh sediments. Geochim. Cosmochim. Acta 58, 1701–1710.

Larsen, O., Postma, D., 2001. Kinetics of reductive bulk dissolution of lepidocrocite, ferrihydrite, and goethite. Geochim. Cosmochim. Acta 65, 1367–1379.

Luther III, G.W., Sundby, B., Lewis, B.L., Brendel, P.J., Silverberg, N., 1997. Interactions of manganese with the nitrogen cycle: Alternative pathways to dinitrogen. Geochim. Cosmochim. Acta 61, 4043–4052.

Mandernack, K.W., Post, J., Tebo, B.M., 1995. Manganese mineral formation by bacterial spores of the marine *Bacillus*, strain SG-1: Evidence for the direct oxidation of Mn (II) to Mn (IV). Geochim. Cosmochim. Acta 21, 4393–4408.

Murray, J.W., Dillard, J.D., Giovanoli, R., Moers, H., Stumm, W., 1985. Oxidation of Mn(II): initial mineralogy, oxidation state and ageing. Geochim. Cosmochim. Acta 49, 463–470.

Myers, C.R., Nealson, K.N., 1988. Bacterial manganese reduction and growth with manganese oxide as the sole electron acceptor. Science 240, 1319–1321.

Nelson, Y.M., Lion, L.W., Ghiorse, W.C., Shuler, M.L., 1999. Production of biogenic Mn oxides by *Leptothrix disophora* SS-1 in a chemically defined growth medium and evaluation of their Pb adsorption characteristics. Appl. Environ. Microbiol. 65, 175–180.

Postma, D., 1985. Concentration of Mn and separation from Fe in sediments – I. Kinetics and stoichiometry of the reaction between birnessite and dissolved Fe(II) at 10°C. Geochim. Cosmochim. Acta 49, 1023–1033.

Postma, D., 1993. The reactivity of iron oxides in sediments: a kinetic approach. Geochim. Cosmochim. Acta 57, 5027–5034.

Postma, D., Jakobsen, R., 1996. Redox zonation: Equilibrium constraints on the Fe(III)/SO_4-reduction interface. Geochim. Cosmochim. Acta 60, 3169–3175.

Puls, W., Sündermann, J., 1990. Simulation of suspended sediment dispersion in the North Sea. In: Cheng, R.T. (Ed.), Residual Currents and Long-Term Transport. Coastal and Estuarine Studies, vol. 38. Springer, New York, pp. 35–372.

Ruttenberg, K.C., 1992. Development of a sequential extraction method for different forms of phosphorus in marine sediments. Limnol. Oceanogr. 37, 1460–1482.

Slomp, C.P., Malschaert, J.F.P., Lohse, L., Van Raaphorst, W., 1997. Iron and manganese cycling in different sedimentary environments on the North Sea continental margin. Cont. Shelf Res. 17, 1083–1117.

Schenau, S.J., 1999. Cycling of phosphorus and manganese in the

Arabian Sea during the late Quaternary. Geologica Ultraiectina 182. Ph.D. Thesis. Utrecht University, Utrecht.

Schulzberger, B., Suter, D., Schiffert, C., Banwart, S., Stumm, W., 1989. Dissolution of Fe(III)(hydr)oxides in natural waters; Laboratory assessment on the kinetics controlled by surface coordination. Mar. Chem. 28, 127–144.

Stone, A.T., Morgan, J.J., 1984. Reduction and dissolution of manganese (III) and (IV) oxides by organics: Survey of the reactivity of organics. Environ. Sci. Technol. 18, 617–624.

Stumm, W., Schulzberger, B., 1992. The cycling of iron in natural environments: Considerations based on laboratory studies of heterogeneous redox processes. Geochim. Cosmochim. Acta 56, 3233–3257.

Sündermann, J., 1993. Suspended particulate matter in the North Sea: field observations and modelling. Phil. Trans. R. Soc. Lond. A 343, 45–52.

Tarutis Jr., W.J., 1993. On the equivalence of the power and reactive continuum models of organic matter diagenesis. Geochim. Cosmochim. Acta 57, 1349–1350.

Thamdrup, B., Glud, R.N., Hansen, J.W., 1994. Manganese oxidation and in situ manganese fluxes from a coastal sediment. Geochim. Cosmochim. Acta 58, 2563–2570.

Van Cappellen, P., Wang, Y., 1996. Cycling of iron and manganese in surface sediments: A general theory for the coupled transport and reaction of carbon, oxygen, nitrogen, sulfur, iron and manganese. Am. J. Sci. 296, 197–243.

Van der Zee, C., Van Raaphorst, W., Epping, E., 2001. Adsorbed Mn^{2+} and Mn redox cycling in Iberian continental margin sediments (northeast Atlantic Ocean). J. Mar. Res. 59, 133–166.

Van der Zee, C., Van Raaphorst, W., Helder, W., De Heij, H., 2003. Manganese diagenesis in temporal and permanent depositional areas in the North Sea. Cont. Shelf Res. 23, 625–646.

Van Raaphorst, W., Kloosterhuis, H.T., Berghuis, E.M., Gieles, A.J.M., Malschaert, J.F.P., Van Noort, G.J., 1992. Nitrogen cycling in two types of sediments of the southern North Sea (Frisian Front, Broad Fourteens): field data and mesocosm results. Neth. J. Sea Res. 28, 293–316.

Van Raaphorst, W., Malschaert, H., Van Haren, H., 1998. Tidal resuspension and deposition of particulate matter in the Oyster grounds, North Sea. J. Mar. Res. 56, 257–291.

Van Weering, T.C.E., Berger, G.W., Kalf, J., 1987. Recent sediment accumulation in the Skagerrak, northeastern North Sea. Neth. J. Sea Res. 21, 177–189.